Inorg. Chem. **2007**, *46*, 9146–9154

A Pnictogen of Peculiar Posture

Anne Poduska and Roald Hoffmann*

Department of Chemistry and Chemical Biology, Baker Laboratory, Cornell University, Ithaca, New York 14853-1301

Received May 7, 2007

In 2001, Bridgeman et al. synthesized a rare species having a T-shaped phosphorus atom centering an organometallic cluster, $[\{Cp(OC)_2Mo\}_2PMn(CO)_4]$. Our DFT and extended Hückel electronic structure calculations indicate that the T-shaped geometry results from an unusual Mo–Mn–Mo three-center, two-electron bond that "ties" back the two-center, two-electron Mo–P bonds. Additional stabilization of the planar structure arises from Mo–P π back-donation in a three-center, four-electron Mo–P–Mo π bond. We find that this compound best resembles a μ_2-phosphinidene system, and we also attempt to reconcile 18- and 8-electron rule considerations with the delocalized bonding in this intriguing cluster.

Introduction

One typically finds neutral tricoordinate phosphorus in pyramidal (C_{3v}) or, more rarely, in locally planar geometries, such as that seen in $(Mes_2B)_2PPh$.[1] Remarkably, a T-shaped phosphorus exists in an organometallic compound, $[\{Cp(OC)_2Mo\}_2PMn(CO)_4]$, shown in Figure 1 and hereafter referred to as PM_3, synthesized by Bridgeman, Mays, and Woods.[2]

Atypical geometries at a transition metal or main group center are often a sign of unusual bonding; this paper will explore the electronic motivations for PM_3 and relate it to μ_2-phosphinidene complexes. As we shall see, the stabilization of this geometry is due to a peculiar 3-center-2-electron (3c2e) Mo−Mn−Mo bond, with additional Mo−P π back-bonding in a 3-center-4-electron (3c4e) π bond.

T-Shaped P in Theory and Experiment. A T-shaped phosphorus center is normally at quite high energy relative to other stereochemical alternatives. Calculations give a cost of around 34 kcal/mol for transformation of pyramidal PH_3 to a planar D_{3h} geometry.[3,4] Widening one of the planar H−P−H angles from 120° to 180°—which consequently causes a 0.20 Å increase in the axial P−H bond length—costs an additional 91 kcal/mol.[3] Thus, the barrier to make

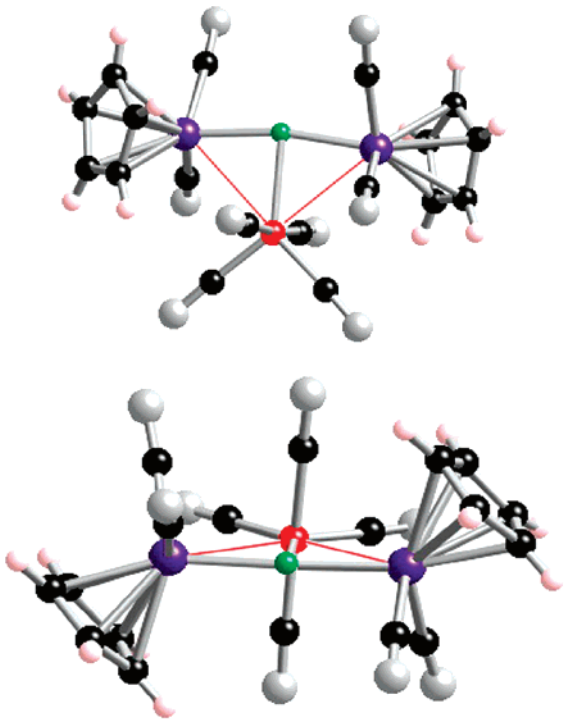

Figure 1. Two views of $[\{Cp(OC)_2Mo\}_2PMn(CO)_4]$ with P = green, Mo = purple, Mn = red, C = black, O = gray, and H = pink.

PH_3 T-shaped (125 kcal/mol) surpasses its mean P−H bond energy (77 kcal/mol).[5] However, theoretical calculations indicate that a T-shaped geometry may play a role as a

* To whom correspondence should be addressed. E-mail: rh34@cornell.edu.

(1) Bartlett, R.; Dias, H. V. R.; Power, P. *Inorg. Chem.* **1988**, *27*, 3919. Nyulaszi, L. *Tetrahedron* **2000**, *56*, 79.
(2) Bridgeman, A. J.; Mays, M. J.; Woods, A. D. *Organometallics* **2001**, *20*, 2932.
(3) Creve, S.; Nguyen, M. T. *J. Phys. Chem. A* **1998**, *102*, 6549.
(4) Grant, D. J.; Dixon, D. A. *J. Phys. Chem. A* **2006**, *110*, 12955.
(5) Greenwood, N. N.; Earnshaw, A. *Chemistry of the Elements*, 2nd ed.; Butterworth-Heinemann: Boston, 1997.

10.1021/ic700881d CCC: $37.00
Published on Web 09/29/2007

transition state in the inversion of molecules such as PF_3 and a saturated P-3-ADPO compound.[6]

On the experimental side, there is a small but expanding family of T-shaped pnictogens, ranging from single molecules to one-dimensional ladders;[7−9] theoretically, there has been an enumeration of T-shaped main group centers in 1-, 2-, and 3-dimensional networks.[10] T-shaped P compounds, however, appear to be quite rare: a Cambridge Structural Database[11] (CSD) search shows that PM_3 appears to be the only T-shaped P compound with phosphorus−transition metal bonds. And apart from the 10-P-3-ADPO compounds with a NPO_2 core,[8,9] the only other T-shaped P compounds are of the type $RePE_2$ (Re = rare earth, E = main group).[12] (None of these compounds, however, have two equivalent angles as seen in PM_3).

Computational Methodology and Calibration. Due to near-degeneracy effects in the first-row transition metal 3d and 4s orbitals, multiple low-energy states are sometimes difficult to compute when using single-configuration methods such as HF and MP2. DFT methods—such as the density gradient-corrected B3[13] functional used in conjunction with correlation functionals LYP,[14] PW91,[15] or P86[16]—are generally more successful at handling near-degeneracy effects in first-row transition metals.[17]

One must be also be mindful of calculations involving phosphorus atoms. Previous work[18] shows that in order to attain basis-set-independent results, it is advantageous to use a large basis set with polarization and electron correlation terms.

Taking these considerations into account, we optimized the experimental geometry of PM_3 and carried out a frequency calculation with the Gaussian 03 program[19] using the B3LYP method. We compared two different basis sets on the transition metals—LANL2DZ,[20] which employs the Los Alamos ECP plus double-ζ, and SDD, which uses the Stuttgart/Dresden ECP[21]—while we used just one basis set, 6-31G*, for the H, C, O, and P atoms. Both calculations gave similar results and showed the T-shape to be a minimum on the potential energy surface. However, LANL2DZ gave a slightly better match with the experimental structure, so we will consider only those results in our analysis.

The P−M bond distances were quite close to the experimental values, with P−Mo at 2.27 Å (0.01 Å too long) and P−Mn at 2.33 Å (0.04 Å too long). The Mn−Mo distance error was much larger (0.11 Å) but was similar to the distance given with the SDD basis set. The T-shaped geometry was maintained, with the Mn−P−Mo angle optimizing within 3° of the experimental value. All other distances were within 2% of the experimental distances, and all optimized bond angles were within 4° of experimental values. The optimized Cartesian coordinates have been included in the Supporting Information. To analyze the bonding, we performed extended Hückel (eH) calculations with the CACAO[22] and YAeHMOP[23] programs.

PM_3: General Features and 18-Electron Rule Considerations. Although the P is atypically coordinated, the $MoCp(CO)_2$ and $Mn(CO)_4$ fragments in this molecule are in fairly conventional geometries. $Mn(CO)_4$ looks like a typical octahedral fragment, albeit somewhat twisted. If one considers Mn−Mo, Mo−P, and Mn−P as single-bonded interactions, Mn might be described as an edge-capped

(6) Dixon, D.; Arduengo, A. *J. Am. Chem. Soc.* **1987**, *109*, 338. Dixon, D.; Arduengo, A.; Fukunaga, T. *J. Am. Chem. Soc.* **1986**, *108*, 2461. Dixon, D. A.; Arduengo, A. J.; Lappert, M. F. *Heteroatom Chem.* **1991**, *2* (5), 541. Arduengo, A. J.; Dixon, D. A.; Roe, D. C. *J. Am. Chem. Soc* **1986**, *108*, 6821.

(7) Arduengo, A.; Lattman, M.; Dias, H. V.; Calabrese, J. C.; Kline, M. *J. Am. Chem. Soc.* **1991**, *113*, 1799. Arney, D. J.; Bruck, M. A.; Huber, S. R.; Wigley, D. E. *Inorg. Chem.* **1992**, *31*, 3749. Chisholm, M. H.; Folting, K.; Huffman, J. C.; Leonelli, J.; Marchant, N. S.; Smith, C. A.; Taylor, L. C. E. *J. Am. Chem. Soc.* **1985**, *107*, (12), 3722. Feasey, N. D.; Knox, S. A. R.; Orpen, A. G. *J. Chem. Soc., Chem. Commun.* **1982**, *75*. Fenske, D.; Godemeyer, T.; Dehnicke, K. *Z. Naturfosch., B: Chem. Sci.* **1988**, *43* (1), 12. Gebeyehu, Z.; Weller, F.; Neumuller, B.; Dehnicke, K. *Z. Anorg. Allg. Chem.* **1991**, *593*, 99. Banaszak Holl, M. M.; Wolczanski, P. T.; Van Duyne, G. D. *J. Am. Chem. Soc.* **1990**, *112*, 7989. Banaszak Holl, M. M.; Wolczanski, P. T.; Proserpio, D.; Bielecki, A.; Zax, D. B. *Chem. Mater.* **1996**, *8*, 2468.

(8) Arduengo, A. J.; Stewart, C. A. *Chem. Rev.* **1994**, *94*, 1215.

(9) Arduengo, A. J.; Stewart, C. A.; Davidson, F.; Dixon, D. A.; Becker, J. Y.; Culley, S. A.; Mizen, M. B. *J. Am. Chem. Soc.* **1987**, *109* (3), 627.

(10) Ienco, A.; Proserpio, D.; Hoffmann, R. *Inorg. Chem.* **2004**, *43*, 2526.

(11) Allen, F. H. *Acta Cryst.* **2002**, *B58*, 380; Bruno, I. J.; Cole, J. C.; Edgington, P. R.; Kessler, M.; Macrae, C. F.; McCabe, P.; Pearson, J.; Taylor, R. *Acta Crystallogr.* **2002**, *B58*, 389.

(12) Tardif, O.; Hou, Z.; Nishiura, M.; Koizumi, T.-a.; Wakatsuki, Y. *Organometallics* **2001**, *20*, 4565. Recknagel, A.; Stalke, D.; Roesky, H. W.; Edelmann, F. T. *Angew. Chem., Int. Ed. Engl.* **1989**, *28* (4), 445.

(13) Becke, A. D. *Phys. Rev. A* **1988**, *38*, 3098; Becke, A. D. *J. Chem. Phys.* **1993**, *98*, 1372. Becke, A. D. *J. Chem. Phys.* **1993**, *98* (7), 5648.

(14) Lee, C.; Yang, W.; Parr, R. G. *Phys. Rev. B* **1988**, *37*, 785. Miehlich, B.; Savin, A.; Stoll, H.; Preuss, H. *Chem. Phys. Lett.* **1989**, *157* (3), 200.

(15) Burke, K.; Perdew, J. P.; Wang, Y. In *Electronic Density Functional Theory: Recent Progress and New Directions*; Dobson, D. F., Vignale, G., Das, M. P., Eds.; Plenum: New York, 1998. Perdew, J. P., *Electronic Structure of Solids ' 91*; Akademie Verlag: Berlin, 1991. Perdew, J. P.; Chevary, J. A.; Vosko, S. H.; Jackson, K. A.; Pederson, M. R.; Singh, D. J.; Fiolhais, C. *Phys. Rev. B* **1992**, *46*, 6671. Perdew, J. P.; Chevary, J. A.; Vosko, S. H.; Jackson, K. A.; Pederson, M. R.; Singh, D. J.; Fiolhais, C. *Phys. Rev. B* **1993**, *48*, 4978. Perdew, J. P.; Burke, K.; Wang, Y. *Phys. Rev. B* **1996**, *54*, 16533.

(16) Perdew, J. P. *Phys. Rev. B* **1986**, *33*, 8822.

(17) Niu, S.; Hall, M. B. *Chem. Rev.* **2000**, *100*, 353. Harrison, J. F. *Chem. Rev.* **2000**, *100*, 679. McCullough, E. A.; Apra, E.; Nichols, J. *J. Phys. Chem. A* **1997**, *101*, 2502.

(18) Gilheany, D. G. *Chem. Rev.* **1994**, *94*, 1339. Marynick, D. S.; Dixon, D. A. *J. Phys. Chem.* **1982**, *86* (6), 914.

(19) Frisch, M. J.; Trucks, G. W.; Schlegel, H. B.; Scuseria, G. E.; Robb, M. A.; Cheeseman, J. R.; Montgomery, J. A., Jr.; Vreven, T.; Kudin, K. N.; Burant, J. C.; Millam, J. M.; Iyengar, S. S.; Tomasi, J.; Barone, V.; Mennucci, B.; Cossi, M.; Scalmani, G.; Rega, N.; Petersson, G. A.; Nakatsuji, H.; Hada, M.; Ehara, M.; Toyota, K.; Fukuda, R.; Hasegawa, J.; Ishida, M.; Nakajima, T.; Honda, Y.; Kitao, O.; Nakai, H.; Klene, M.; Li, X.; Knox, J. E.; Hratchian, H. P.; Cross, J. B.; Bakken, V.; Adamo, C.; Jaramillo, J.; Gomperts, R.; Stratmann, R. E.; Yazyev, O.; Austin, A. J.; Cammi, R.; Pomelli, C.; Ochterski, J. W.; Ayala, P. Y.; Morokuma, K.; Voth, G. A.; Salvador, P.; Dannenberg, J. J.; Zakrzewski, V. G.; Dapprich, S.; Daniels, A. D.; Strain, M. C.; Farkas, O.; Malick, D. K.; Rabuck, A. D.; Raghavachari, K.; Foresman, J. B.; Ortiz, J. V.; Cui, Q.; Baboul, A. G.; Clifford, S.; Cioslowski, J.; Stefanov, B. B.; Liu, G.; Liashenko, A.; Piskorz, P.; Komaromi, I.; Martin, R. L.; Fox, D. J.; Keith, T.; Al-Laham, M. A.; Peng, C. Y.; Nanayakkara, A.; Challacombe, M.; Gill, P. M. W.; Johnson, B.; Chen, W.; Wong, M. W.; Gonzalez, C.; Pople, J. A. *Gaussian 03*, revision C.02; Gaussian, Inc.: Wallingford, CT, 2004.

(20) Hay, P. J.; Wadt, W. R. *J. Chem. Phys.* **1985**, *82* (1), 270. Hay, P. J.; Wadt, W. R. *J. Chem. Phys.* **1985**, *82* (1), 299. Wadt, W. R.; Hay, P. J. *J. Chem. Phys.* **1985**, *82*, (1), 284.

(21) Dolg, M.; Stoll, H.; Preuss, H.; Pitzer, R. M. *J. Phys. Chem.* **1993**, *97*, 5852. Dolg, M.; Wedig, U.; Stoll, H.; Preuss, H. *J. Chem. Phys.* **1987**, *86*, 866.

(22) Mealli, C.; Proserpio, D. M. *J. Chem. Ed.* **1990**, *67* (5), 399.

(23) http://yaehmop.sourceforge.net/.

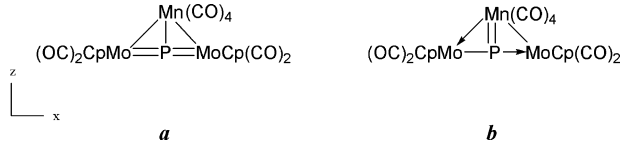

Figure 2. Two 18-electron bonding schemes for PM_3. There are several resonance structures for (b).

octahedron. If one regards $CpMo(CO)_2$ as bonding only to P, the Mo geometry is typical of $CpML_3$ entities.

Ignoring any metal−metal and metal−phosphorus bonding, electron counting then gives two Mo(I), 15-electron $MoCp(CO)_2$ fragments and a Mn(0), 15-electron $Mn(CO)_4$ fragment. Thus, the 18-electron rule could be satisfied for the Mn fragment by forming two Mo−Mn bonds and one Mn−P single bond. For each Mo (see Figure 2a), one Mo−Mn single bond and a Mo−P double bond would be necessary to reach 18 electrons. The resulting five bonds to P are unusual, to put it mildly. Another 18-electron-rule obeying structure, this time with a P−Mn double bond and two dative bonds, was suggested to us by P. T. Wolczanski. This is shown in Figure 2b.

Let us look at the bond distances next. As Bridgeman et al. noted, the P−Mn distance, 2.28 Å, is within single-bond range[23,24] (the covalent radii for P and Mn are 1.10 and 1.17 Å, respectively) and Mn═P double bonds appear around 2.10 Å.[25] The Mo−Mn distance of 3.07 Å, however, is somewhat long (as compared to the sum of atomic radii, 2.47 Å) but comparable to reported Mo−Mn single-bond lengths, which range from 2.99 to 3.10 Å, depending on the presence of bridging ligands.[25−27] Thus, it is not immediately obvious to us what bond order the Mo−Mn bond length indicates.

As we noted, one application of the 18-electron rule leads one to postulate a P−Mo double bond in addition to the Mo−Mn single bond (Figure 2a). The P−Mo distance of 2.26 Å is indeed substantially shorter than the single-bond range 2.40−2.57 Å reported by Cowley et al.[28] and the atomic radii sum (2.40 Å). Compounds with some measure of multiple bonding appear to be in the 2.20−2.30 Å range,[29] but the delineation of a particular bond order in this range is unclear.

The other plausible 18-electron-rule structure (Figure 2b) draws a Mn−P double bond. There is no sign in the observed distance of 2.28 Å of multiple bonding, however. Calculations (to be reported below) show very little Mn−P π bonding, so this structure also does not appear consistent with bond lengths in PM_3.

The Unusual Nature of PM_3. To gain an appreciation for how odd the PM_3 molecule is, we can use the isolobal analogy[30,31] to relate PM_3 to main-group analogues. The d^7 $Mn(CO)_4$ fragment is isolobal with CH_2^+. The d^5 ML_5 fragment $MoCp(CO)_2$ is isolobal with CH_3^{2+}, or, if one uses the deprotonation analogy,[30] with CH_2^+ or CH. Recognizing that P is isovalent with CH_2^+, $[\{Cp(OC)_2Mo\}_2PMn(CO)_4]$ is transformed into an electron-deficient bicyclobutane derivative, $C_4H_6^{2+}$. Moreover, noting that CH is also isovalent with P, we can also relate PM_3 to P_4—which is hardly a molecule that would be expected to harbor a planar T-shaped atom.

Another analogy with main-group compounds—this time with main-group T-shapes—also presents us with a puzzle. While the structural details of PM_3 implicates P−Mo multiple bonding, as shown in Figure 2a, the Mo−P−Mo axis geometrically resembles the "axial" bond set of a T-shaped molecule, and in main group models, that axis is the locus of electron-rich three-center bonding, which in turn is weaker than normal two-center bonding. Therefore, the axial bonds in BrF_3 are 1.81 Å, while the equatorial bond is 1.72 Å,[32] but in our T-shaped PM_3, our axial bonds (2.26 Å) are shorter than the equatorial bond (2.28 Å). As we will discuss later, this quandary is best resolved if we consider PM_3 to be analogous to a μ_2-phosphinidene fragment, not a main-group T-shaped molecule.

Building up PM_3. To understand the electronic factors operating in this uncommon geometry, we employ the fragment molecular orbital (FMO) approach, first assembling the transition metal fragments, then interacting them with the P. Our analysis will not end with our FMO diagram, however, for we would like to relate the 18-electron rule considerations to the delocalized molecular orbitals. This is not done all that often: application of the 18-electron rule typically concludes by noting whether the rule is satisfied (or not) and correlating the resulting bond order with bond length. In this particular case, the explicit connection of orbitals with bonds is also a difficult task, given the large amount of mixing and the great number of orbitals in PM_3.

Although electronics are presumably the primary stabilizing force behind this T-shape, sterics are also a consideration. Repulsions between carbonyls and also between carbonyls and Cp's restrict the Mn−P−Mo angle to the 79−119° range; a butterfly-type distortion from planarity is allowed up to 11.5°. Please consult the Supporting Information for a more detailed discussion on the steric restrictions in PM_3.

The frontier orbitals of $MoCp(CO)_2$ and $Mn(CO)_4$ are well known[33] and are shown in Figure 3a and b. $MoCp(CO)_2$ is formally isolobal to a d^5 ML_5 fragment, and Figure 3a shows that the "t_{2g}" set is occupied by five electrons, above which

(24) Veiros, L. F. *Organometallics* **2000**, *19* (16), 3127. Enemark, J. H.; Ibers, J. A. *Inorg. Chem.* **1967**, *6*, 1575.
(25) Lang, H.; Leise, M.; Emmerich, C. *J. Organomet. Chem.* **1991**, *418* (1), C9.
(26) Bir'yukov, B. P.; Struchkov, Y. T. *Zh. Strukt. Khim. (Russ.) (J. Struct. Chem*) **1968**, *9* (4), 655. Doedens, R. J.; Robinson, W. T.; Ibers, J. A. *J. Am. Chem. Soc.* **1967**, *89* (17), 4323.
(27) Bir'yukov, B. P.; Struchkov, Y. T.; Anisimov, K. N.; Kolobova, N. E.; Beschastnov, A. S. *Chem. Commun. (London*) **1968**, *12*, 667.
(28) Cowley, A. H.; Giolando, D. M.; Nunn, C. M.; Pakulski, M.; Westmoreland, D.; Norman, N. C. *J. Chem. Soc., Dalton Trans.* **1988**, 2127.
(29) Cherry, J.-P. F.; Stephens, F. H.; Johnson, M. J. A.; Diaconescu, P. L.; Cummins, C. C. *Inorg. Chem.* **2001**, *40*, 6860. Garcia, M. E.; Riera, V.; Ruiz, M. A.; Saez, D.; Hamidov, H.; Jeffery, J. C.; Riis-Johannessen, T. *J. Am. Chem. Soc* **2003**, *125*, 13044. Mosch-Zanetti, N. C.; Schrock, R. R.; Davis, W. M.; Wanninger, K.; Seidel, S. W.; O'Donoghue, M. B. *J. Am. Chem. Soc.* **1997**, *119*, 11037. Sanchez-Nieves, J.; Sterenberg, B. T.; Udachin, K. A.; Carty, A. J. *Inorg. Chim. Acta* **2003**, *350*, 486.
(30) Hoffmann, R. *Angew. Chem., Int. Ed. Engl.* **1982**, *21* (10), 711.
(31) Hoffmann, R. *Science* **1981**, *211* (4486), 995.
(32) Albright, T. A.; Burdett, J. K.; Whangbo, M. H. *Orbital Interactions in Chemistry*; John Wiley and Sons: New York, 1985.
(33) Elian, M.; Hoffmann, R. *Inorg. Chem.* **1975**, *14* (5), 1058. Schilling, B. E. R.; Hoffmann, R.; Lichtenberger, D. L. *J. Am. Chem. Soc.* **1979**, *101* (3), 585.

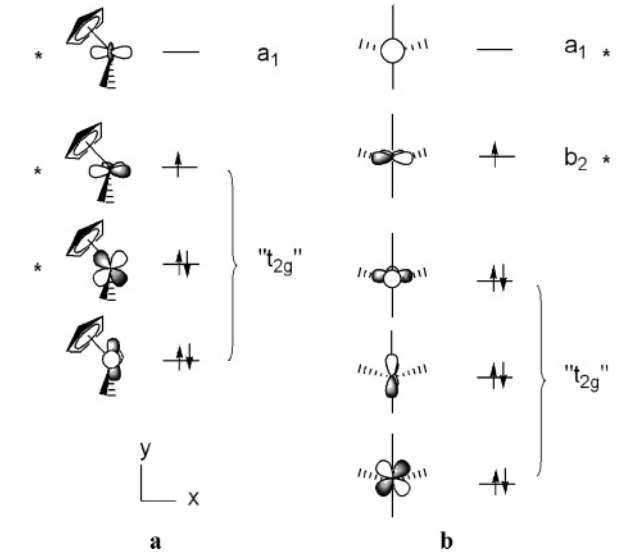

Figure 3. Valence orbitals of $MoCp(CO)_2$ and $Mn(CO)_4$. The MOs that are significant contributors to framework bonding are marked with an asterisk.

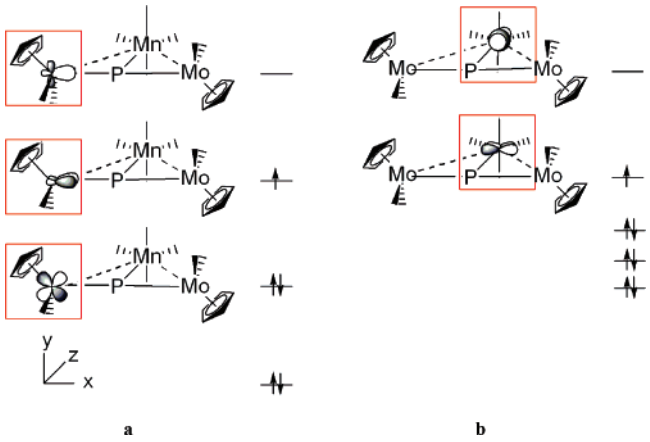

Figure 4. Frontier orbitals of (a) one $MoCp(CO)_2$ and (b) $Mn(CO)_4$, looking down the *z* axis. The lowermost d orbitals from Figure 3 for both transition metal fragments are shown schematically.

lies an important hybrid orbital a_1. $Mn(CO)_4$ is a typical d^7 ML_4 fragment; its valence orbitals are shown in Figure 3b. Above a "t_{2g}" set, one has valence orbitals (a_1 and b_2) that are symmetric and antisymmetric with respect to the *yz* plane.

Only the orbitals in Figure 3 marked with an asterisk figure significantly in M−P and M−M bonding. The lowest member of the t_{2g} set for each Mo does not have the right (pseudo)symmetry to interact with P levels, whereas the three Mn "t_{2g}" orbitals are primarily involved in CO backbonding. Figure 4 shows the valence orbitals we find important, redrawing them still schematically but now in a perspective view.

Preparing the Metal Moiety. To build PM_3, we will interact a P atom with the $Mn(CO)_4$ and two $CpMn(CO)_2$ fragments. The construction is not simple, for there are many orbitals and little symmetry. We ask the reader to bear with us, for there is something interesting at the end, something rare in organometallic chemistry.

To begin, the interaction of the metal fragments requires some preparation by itself. A "top" view of two $MoCp(CO)_2$ is shown in Figure 5a; a similar view of the $Mn(CO)_4$ valence orbitals is shown in Figure 5b. Two $MoCp(CO)_2$ units carry 10 d electrons in eight valence orbitals. As we argued above, one occupied orbital per Mo is "inactive", ergo the six electrons in six orbitals in Figure 5a. Similarly, for the $Mo(CO)_4$ fragment, the six electrons in the t_{2g} set are "inactive" in M−P bonding, leaving one electron in the two frontier orbitals in Figure 5b. The P atom brings in five electrons in its four valence orbitals. Thus, there will be a total 12 valence-active electrons in PM_3.

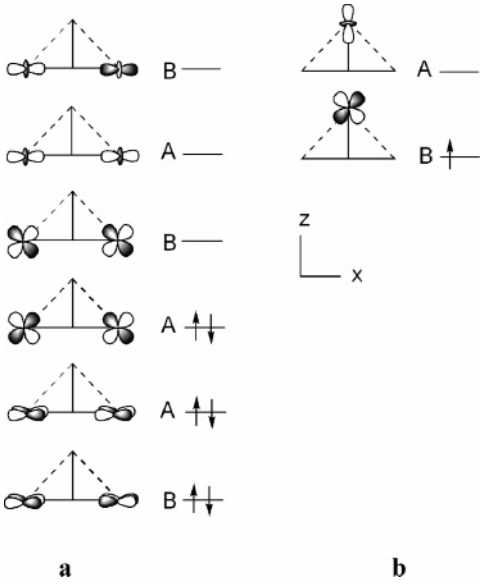

Figure 5. Top view of the important frontier orbitals of two $MoCp(CO)_2$ and $Mn(CO)_4$ fragments. The group-theoretical labels "A" and "B" identify the MO as symmetric or antisymmetric with respect to the C_2 (*z*) axis.

Interacting the Fragments. When we interact these metal fragment orbitals, we get the molecular orbitals at the left of Figure 6. At the right in Figure 6 are the relevant P orbitals. The composite molecule MOs, or a selection of the important ones of these (see text that follows), are shown in the middle column. In what follows, we will analyze the σ interaction (consisting of orbitals mainly in the *xz* plane) and the π system (composed of orbitals mainly perpendicular to the *xz* plane). The reason why we say "mainly" is that, in the low C_2 symmetry of PM_3, the σ and π orbitals mix.

There are 145 MOs in the extended Hückel calculation on the molecule, so how can we get at those that are essential to the P−M core bonding? We looked at the contributions to the total Mo−P, Mn−P, and Mo−Mn Mulliken overlap populations, orbital by orbital. Even though there is substantial mixing, so that both M−P σ and π character are washed out over several orbitals, it is possible to identify orbitals that are involved in an essential way in bonding in the PM_3 core. Those are shown in Figure 6; the less important orbitals have generally been omitted. For instance, there are no fewer than 24 levels between the π and B2 orbitals, which contribute very little to PM_3 bonding. They are mostly on the Cp's or are involved in Mo−Cp and Mn−Cp bonding and are not shown in Figure 6. Two fairly noninteracting Mo d orbitals that come below the π nonbonding orbital are also omitted from the figure. Below all of these orbitals are

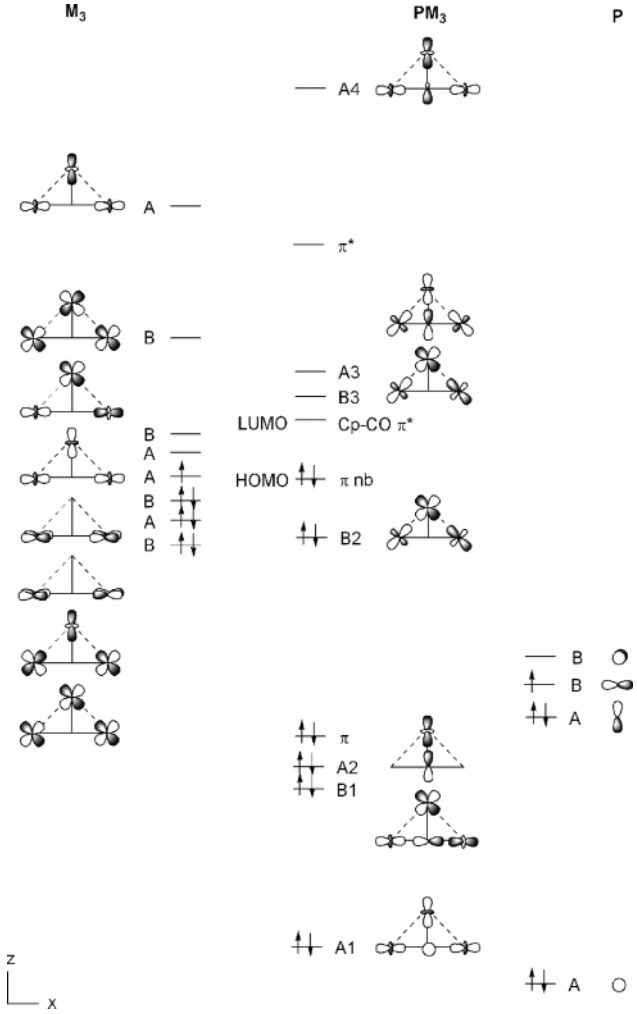

Figure 6. Schematic molecular orbital diagram of PM_3 looking down the *y* axis. 10 mainly d electrons in five levels are not shown at left, and many orbitals of the composite PM_3 molecule (middle) are omitted for clarity. See text for further discussion.

the A1, A2, B1, and π orbitals, primarily responsible for the σ and π bonding in the molecule. We will return to these presently, but one first needs to address an obvious question: in a system as complicated as this molecule, are the orbitals sensitive to the theoretical methodology?

We examined PM_3 with both DFT and eH calculations, the latter less reliable in a number of ways, yet easier to analyze. In the Supporting Information, we show an eH−DFT comparison of the bonding levels and energies. In general, the energy level ordering is maintained, apart from a flipping of the A3 and B3 orbital, which is likely due to their small separation (0.18 eV with DFT, 0.21 eV with eH). There is one significant difference between DFT and eH, though, which we will delve into later: in DFT, the LUMO is the π* level with a large P coefficient, whereas this MO is the LUMO+18 in eH and has lobes mainly localized on the Mo atoms.

σ-Bonding. Returning to our eH results in Figure 6, we would like to identify the three lowermost orbitals—A1, B1, A2—as the main contributors to the M−P σ bonding, fully aware of the simplifications implicit in such an assignment. We pick these orbitals for the following reasons. First, the

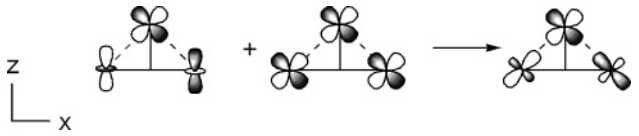

Figure 7. In-phase combination of the Mo d_{z^2} and d_{xz} orbitals to produce the HOMO of PM_3.

Table 1. Total Reduced Overlap Populations and the Important Contributions to the Overlap Population from MOs B1, B2, and A1−A4 and the Mo−P π System

	Mo−P (one)	Mn−P	Mo−Mn
total	0.759	0.377	0.065
A4	0.066	−0.518	−0.097
A3	−0.054	0.051	−0.055
B2	0.014	−0.033	0.050
A2	0.024	0.075	−0.002
B1	0.094	0.015	0.004
A1	0.107	0.047	0.006
	Mo−P		
total	0.759		
π*	−0.104		
π nonbonding	−0.001		
π	0.055		

delocalized equivalents of three localized P−M σ bonds should have symmetries 2A + B. As the schematic drawing of Figure 6 shows, MO B2 (the orbital above the π bonding orbital) is not much involved in M−P σ-bonding. In contrast, the σ-bonding in A1, B1, and A2 is apparent; we can also directly gauge the contributions of these orbitals to M−P bonding, shown in Table 1a, which shows the contributions of various frontier orbitals to bonding in the PM_3 core. Each of these MOs contributes substantially to M−P bonding. The remainder of the σ bonding in PM_3 is distributed over a number of lower-lying orbitals; no single orbital makes as large of a contribution as A1, A2, and B1.

Electron-Deficient Bonding in the Mo−Mn−Mo System. There is one more filled σ-type bonding orbital: B2. The Mo orbitals in B2 appear to be mixtures of two d orbitals, and indeed they are—Figure 7 shows the Mo d_{z^2} and d_{xz} mixing in the low C_2 symmetry.

The B2 orbital, as its composition implies, is a major contributor to Mn−Mo (but not M−P) bonding. As Table 1 shows, the total Mn−Mo overlap population is 0.065, and of this value, the B2 orbital contributes the majority, 0.050. The small total metal−metal OP may be startling at first sight, but in general, such M−M OPs are 5 to 10 times smaller than main-group−main-group overlap populations. Our OP for PM_3, however, is smaller than the Mn−Mn reduced overlap population of 0.140 in $(CO)_5Mn-Mn(CO)_5$[34] and 0.105 in $Cp(CO)_3Mo-Mn(CO)_5$[27] (which has a Mn−Mo distance identical to that of PM_3), both models for a full M−M single bond.

Orbital B2 is actually the single MO with any substantial Mo−Mn bonding. Given the isolated nature of this orbital and its shape, we were reminded of a classical main-group bonding motif, the electron-poor 3c2e bond found, for instance, in boranes.

Let us trace our analogy in more detail. Figure 8a shows the three MOs of a B−H−B unit in diborane. In this system,

(34) Dahl, L. F.; Rundle, R. E. *Acta Crystallogr.* **1963**, *16*, 419.

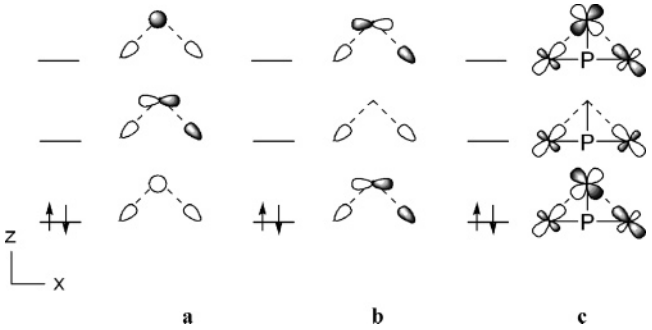

Figure 8. (a) Typical 3c2e bonding system with a central atom s orbital, (b) the three-center bonding orbitals for three main group elements, the central atom now contributing a p orbital, and (c) the 3c2e Mo−Mn−Mo bond in PM_3.

the central atom brings into bonding only an s orbital, symmetric with respect to a *yz* mirror plane. In PM_3, however, the shape of the B2 orbital shows that an antisymmetric orbital at Mn, d_{xz}, is involved. Indeed, in the main group realm, three-center bonds may form with a central atom contributing an antisymmetric p_x orbital to the bonding. This is schematically shown in Figure 8b; realizations are actually not easy to come by, as any realistic main group bridging atom has both s and p orbitals involved in bonding.[35]

Now we will examine PM_3 in the context of these bonding schemes. Instead of a main-group bridging p_x orbital, we substitute in the Mn d_{xz} orbital, whose mode of bonding (in a bent geometry) resembles a p_x orbital. Paying attention to the electron count, we have two electrons available for B2. This is because we have three M−P σ bonds (as mentioned earlier) and a 3c4e π bond (to be discussed in a moment), for a total of 10 electrons. P donates five electrons, so the other five electrons come from M_3. However, we have seven valence electrons on the left-hand side of Figure 6: these two extra electrons go into the 3c2e Mo−Mn−Mo bond.

The actual orbitals that we see in PM_3 are modified from the schematic ones in Figure 8c by substantial mixing with σ-bonding MOs (such as the ones that make up A1, B1, and A2). Changes in energy follow. The closest that we can come to the nonbonding and highest orbital of Figure 8c, the idealized 3c2e scheme with a centering $Mo(CO)_4$, is to identify these with unfilled orbitals A3 and B3.

Although 3c2e bonding is more common in main-group elements, there has been a report of a "closed" (cyclic) 3c2e bond in a $[M_3O_9]^{2-}$ cluster (M = W, Mo),[36] consisting of a hexagonal ring with alternating $O-MO_2$ bonds. The neutral complex has a Mo−Mo distance of 3.53 Å, but upon addition of two electrons, the distance decreases to 3.08 Å, indicating formation of a 3c2e Mo_3 bond. 3c2e transition metal cyclic bonding has also been invoked by King in clusters such as $Os_3(CO)_{12}$.[37]

Electron-Rich Three-Center π Bonding in PM_3. The π bonding in PM_3 also has some interesting features. Into that π bonding enter d_{xy} orbitals on Mo and the p_y on P. The Mn d_{yz} will also mix in to a lesser degree because of Mn−CO π bonding, so we do not show it in the interaction diagram of Figure 9; in the three π orbitals we focus on, the Mn contribution to the overall electron density is 1% or less.

Looking at the interaction diagram in Figure 9, we see a 3c4e Mo−P−Mo π bond (or a metalloorganic analogue of an allyl π system). In the full MO diagram shown in Figure 6, the lowermost component of the 3c4e P−Mo π bond lies above A2, the HOMO is the nonbonding filled orbital of the 3c4e π bond, and the π^* orbital comes above A3.

On the face of it, we have a typical 3c4e bonding situation here, but we are faced with a complication—a difference in the composition of the orbitals, depending on the theoretical method used. First, the most marked difference between DFT and eH calculations in the energies of the frontier orbitals occurs for the π orbitals, and in particular, for π^*. π^* is the LUMO of PM_3 in the DFT calculation but is much higher in energy in the eH calculation. (Please see the comparison of DFT and eH levels in the Supporting Information). Furthermore, the composition of the π MOs (except π nonbonding) is method dependent, as Table 2 shows.

Notice the difference in the composition of π and π^*. We are inclined to accept the results of the DFT calculations as being more reliable, which has the largest P p_y contribution in the unfilled highest orbital, the LUMO of PM_3, which we called π^*. Thus, it appears that the P p_y orbital is empty and the important conclusion, independent of method, is that the 3c4e bonding we see adds a π component to the Mo−P bonding.

As with the PM_3 σ system, we show in Table 1 the contributions of the three Mo−P π orbitals to the reduced overlap population (from an eH calculation). The π-bonding orbital has the highest contribution to the Mo−P OP, apart from the 2A + B σ-bonding orbitals (and a low-lying orbital that has some Mo−P overlap due to the large amount of mixing in this complicated molecule). The π bonding, with its 3c4e character, does not add two full Mo−P bonds, as a naïve 18-electron rule interpretation would have it. It does strengthen Mo−P bonding, consistent with the P−Mo distance that is intermediate between a single and a double bond.

Phosphinidene-Type Bonding in PM_3. A 3c4e π bond has also been postulated for transition metal-bridging phosphinidene (μ_2-PX) fragments.[28,38−40] The P π lone pair is taken as empty, as all of the phosphinidene electrons are involved in the σ system. In these complexes, P is a one-electron donor to X and a two-electron donor to its two other substituents (see Figure 10).

As in PM_3, the empty P π orbital is filled due to π back-donation from the two transition metals: calculations on $[CpMn(CO)_2]_2PPh$[41] show substantial π back-donation (0.33 electrons) from Mn to the empty P p orbital in the 3c4e π bond. Since the empty π^* component is has a large P

(35) Munzarova, M. L.; Hoffmann, R. *J. Am. Chem. Soc.* **2002**, *124*, 4787.
(36) Huang, X.; Zhai, H. J.; Boggavarapu, K.; Wang, L. S. *Angew. Chem., Int. Ed.* **2005**, *44* (44), 7251.
(37) King, R. B. *Inorg. Chim. Acta* **2003**, *350*, 126.
(38) Arif, A. M.; Cowley, A. H.; Pakulski, M.; Thomas, G. J. *Polyhedron* **1986**, *5* (10), 1651.
(39) Huttner, G.; Evertz, K. *Acc. Chem. Res.* **1986**, *19*, 406.
(40) Ellis, B. D.; Macdonald, C. L. B. *Coord. Chem. Rev.* **2007**, *251*, 936.
(41) Kostic, N. M.; Fenske, R. F. *J. Organomet. Chem.* **1982**, *233* (3), 337.

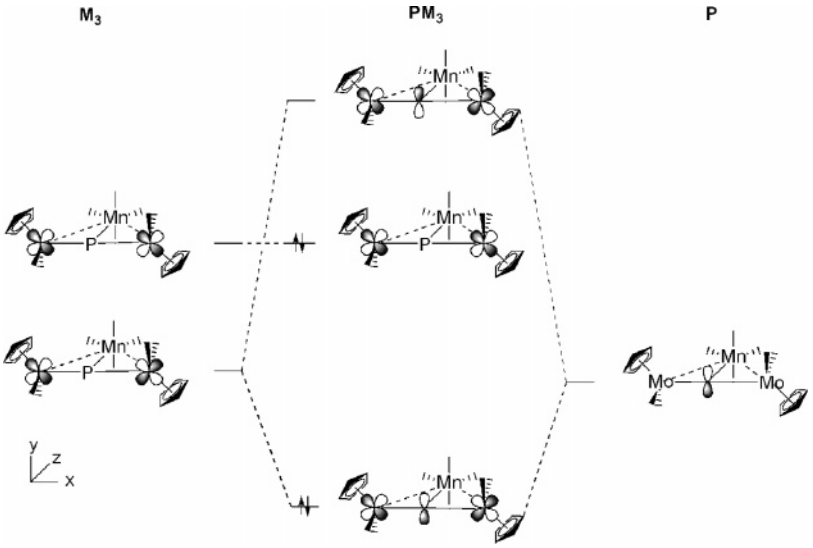

Figure 9. Schematic molecular orbital diagram for the π-only system of PM_3. We have refrained from assigning electrons to the fragment molecular orbitals and instead show only the final orbital filling of PM_3, as given in Figure 6.

Table 2. P p_y and Mo d_{xy} Wavefunction Coefficients (Absolute Values) in DFT and eH Calculations of PM_3[a]

	DFT		eH	
	P	Mo	P	Mo
π*	0.46	0.27	0.37	0.44
π nonbonding	0.00	0.45	0.00	0.52
π	0.24	0.26	0.52	0.10

[a] The actual signs of the molecular orbital coefficients are those shown in Figure 9, middle.

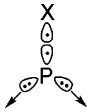

Figure 10. Electron-donating ability of P in a doubly bridging phosphinidene fragment. The P is formally a five-electron donor, donating one electron in one p orbital and two electrons apiece from the s and other in-plane p orbital.

coefficient, such as in $[Cp(CO)_3Mo]_2\mu$-PCl,[42] this makes Lewis base addition at P favorable in phosphinidene complexes.[39]

This similarity suggests that we can also consider P as a five-electron σ donor in PM_3. Further corroboration is provided by the similar Mo−P distances in PM_3 (2.26 Å) and in the phosphinidene complex $[Mo_2(CO)_4Cp_2\{\mu$-P(2,4,6-(t-Bu)$_3C_6H_2$)$\}]$[38] (2.30 Å). Moreover, the sp^2 depiction of P in Figure 10 is consistent with our assertion of three P−M 2c2e bonds in PM_3 and also that the 3c2e Mo−Mn−Mo bond is the primary stabilizing force in this molecule—not a 3c4e Mo−P−Mo σ bond. It is this 3c2e bond which "pulls" the Mo's back toward the Mn, bending the phosphinidene-like P−Mo (formally dative) bonds.

This connection with μ_2-phosphinidenes could give us clues about its potential reactivity. For example, Huttner and Evertz[39] propose that such a 3c4e π bond could exhibit allylic-type ligand properties. One Mo−P π bond in $[\{MoCp(CO)_2\}_2(\mu$-PR)] (R = 2,4,6-$C_6H_2{}^tBu_3$) has been activated under UV to undergo alkyne insertion, as well as intramolecular C−H oxidative addition.[43] This phosphinidene complex can also undergo decarbonylation and halogenation at the Mo centers while still maintaining the phosphinidene bridge. Similar insertion reactions with the M−P bond have also been observed with $[\{Mn(CO)_4\}_2(\mu$-PR)] (R = N^iPr_2): reactions with organic azides and diphenyldiazomethane (Ph_2CN_2) gives an unusual μ-η^1,η^2-aminophosphaimine ligand and Mn_2PN_2 ring, respectively.[44] Perhaps the unusual T-shape of PM_3 might make the P−Mo bond more accessible for similar insertion reactions, as well as for formation of new P−M heterocycles.

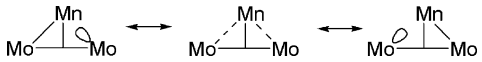

Figure 11. Possible resonance structures for the Mo−Mn−Mo 3c2e bond.

In addition to the Mo−P multiple bond, the T-shaped P also could serve as a center of reactivity. For example, the T-shaped P in 10-P-3-ADPO[8] gives adducts with transition metal centers (encompassing Group 6, 7 ,8 ,10, and 11 metals) to form a tetrahedral geometry at the P, and other phosphinidenes also undergo addition of organometallic nucleophiles at the main group center.[39] Moreover, a trigonal planar As compound, $\{CpMo(CO)_2\}As\{Cr(CO)_5\}_2$, when treated with Ph_3P, eliminates one $Cr(CO)_5$ unit to give a $Cp_2M_2(CO)_2(\mu_2$-η^2-$As_2)$ complex. These findings suggest that PM_3 might be a fruiful starting point for forming larger organometallic clusters, perhaps with bridging P_2 units.

There is little guidance in the literature for thinking about reactivity of the 3c2e Mo−Mn−Mo bond. What comes to mind are the "classical" resonance structures in Figure 11. These imply the potential availability of an acceptor orbital on the Mo components, which could react with a Lewis base.

(42) Grossbruchhaus, V.; Rehder, D. *Inorg. Chim. Acta* **1990**, *172* (2), 141.

(43) Esther Garcia, M.; Riera, V.; Ruiz, M.; Saez, D.; Vaissermann, J.; Jeffery, J. *J. Am. Chem. Soc* **2002**, *124*, 14304.

(44) Graham, T. W.; Udachin, K. A.; Carty, A. J. *Chem. Comm.* **2005**, 4441.

(45) Adams, R.; Captain, B.; Kwon, O.; Miao, S. *Inorg. Chem.* **2003**, *42*, (3356−3365).

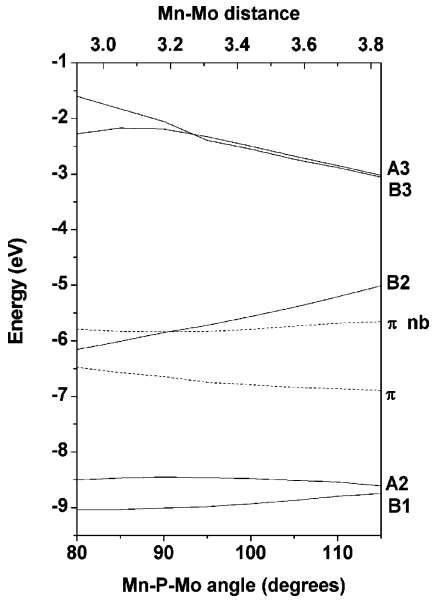

Figure 12. Walsh diagram for widening the Mn−P−Mo angle from 80° to 115° in PM_3. The M−P π orbitals are represented by the dashed lines, whereas the M−P σ core orbitals are represented by the solid lines. The π nonbonding orbital is the HOMO of PM_3.

Support for the Unusual Mo−Mn−Mo Bonding. The Mo−Mn−Mo 3c2e bond is perhaps the most interesting outcome of our tracing of the bonding in PM_3. To convince ourselves that the 3c2e bond is a significant contributor to the bonding in this molecule, we studied a perturbation that tunes the overlap behind this bonding mode. A Walsh diagram in Figure 12 shows the (DFT) energetic changes in widening the Mn−P−Mo angle from 80° to 115°. As in Figure 6, all of the significant M−P σ and π interactions are shown, except for A1, A4, and π*. This Walsh diagram is also complicated by both level and avoided crossings with orbitals not shown here; however, the essence of the M−P bonding is still captured.

There is a minor shifting of the P−Mn and P−Mo σ levels (less than 0.3 eV) in the two lowermost orbitals and also small changes in the π orbitals (from 0.13 eV in the π nonbonding orbital up to 0.42 eV in the π bonding orbital) as the Mn−P−Mo angle increases, likely due to the mixing in this unsymmetric molecule. Clearly B2, B3, and A3 are most affected by changing the Mo−P−Mn angle, with an overall increase of 1.15 eV in the 3c2e bonding orbital, B2. These are the orbitals we have identified as forming a Mo−Mn−Mo 3c2e bonding system, and that bonding is most affected by Mo−Mn separation, a necessary consequence of Mo−P−Mn angle variation. This observation, in conjunction with the large contribution of B2 to the Mo−Mn overlap population, indicates that this Mo−Mn−Mo 3c2e bond is an important contributor to the T-shaped geometry.

Back to the 18-Electron Rule. As we saw during the course of our story, PM_3 is hardly a typical 18-electron organometallic compound. The T-shaped geometry at P in PM_3 by itself is indeed a hint of an unusual underlying electronic structure in this molecule, and there is no consistent precedent in the literature for melding multicenter bonding of the kind we find in PM_3 (an inherently delocalized view of bonding) with the 18-electron rule (an atom-centered view of bonding). Nevertheless, let us see how close we can bring the two views together.

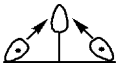

Figure 13. Donation of one electron by each Mo to Mn in the 3c2e bond.

First, the electronic structure we deduce from our MO calculations is inconsistent with both 18-electron-rule valence structures adumbrated (Figure 2). The structure with two P═Mo double bonds (Figure 2a) is not consistent with the length and bonding considerations. The absence of Mn−P π bonding and the clear identification of a 3c2e Mo−Mn−Mo bond are inconsistent with structures of the type shown in Figure 2b.

Let us try to see how far we get with 18-electron rule considerations that are consistent with our delocalized MO picture. We start out with 15-electron $MoCp(CO)_2$ and $Mn(CO)_4$ fragments and five electrons on P. For the σ system, we follow the phosphinidene bonding mode: P is a one-electron donor to Mn (bringing it to 16 electrons) a two-electron donor to both Mo's (these Mo's then reaching 17 electrons). In this analysis, P only gains one electron from the P−Mn bond, i.e., the P has six valence electrons.

Since we have used up six electrons in these three M−P σ bonds (covalent or dative), six active electrons remain (see Figure 6). As we have argued, they are in a Mo−Mn−Mo 3c2e bond and a Mo−P−Mo 3c4e bond—and since P has already donated all of its electrons to Mn and Mo, these six electrons reside formally on the transition metals.

We reach an electron count of 18 at Mn if we consider both Mo's to be one-electron donors in the 3c2e bond (see Figure 13). This still leaves Mo at 17 electrons and the P at six electrons, however. Apportioning the electrons in the 3c4e π bond is tricky: the Mo−P π back-donation can give P two additional electrons to satisfy the octet rule, but the Mo has not gained any additional electrons in this process.

We are stuck at this point with 18 electrons at Mn, 8 electrons at P, and 17 electrons at each Mo. This is as come close as we can come to satisfying the 18-electron rule. Is there an implication of electron-deficiency in PM_3 in this departure from 18 and 8 electrons? Certainly PM_3 has several relatively low-lying empty orbitals, consistent with unsaturation. We are hesitant to identify these definitely as harbingers of unsaturation.

As we have seen, the articulation of the bonding in PM_3 has proven difficult with the traditional lexicon of the 18-electron rule. We have tried to reconcile the highly delocalized orbitals of PM_3 with simple bonding pictures and came to an unexpected role for three-center bonding.

More than that, the electronic structure of this unusual molecule may be a starting point for creating more stories—stories centering on the unusual 3c2e transition metal bonding motif, as well as its similarity to μ_2-phosphinidene compounds. Future studies could explore other T-shaped molecules with 3c2e transition metal bonds and connect them in multidimensional networks.

Acknowledgment. We are grateful to the National Science Foundation in support of this work through Grants No. CHE-0204841 and CHE-0613306. A.P. thanks Daniel Fredrickson for the innumerable discussions and the use of his computational programs. We thank Peter Wolczanski for his comments on our work. Also, during A.P.'s time at the Jawaharlal Nehru Centre for Advanced Scientific Research, she is indebted to Prof. Swapan Pati for the use of his computational resources in preparing this manuscript.

Supporting Information Available: Listings of optimized Cartesian coordinates, energy levels, and steric considerations. This material is available free of charge via the Internet at http://pubs.acs.org.

IC700881D